International Journal of Fracture 31: 245–258 (1986)

An improved analysis of the potential drop method for measuring crack lengths in compact tension specimens

MARK E. ORAZEM [1] and WOLFGANG RUCH [2]

[1] *Department of Chemical Engineering, University of Virginia, Charlottesville, VA 22901, USA*
[2] *Department of Materials Science, University of Virginia, Charlottesville, VA 22901, USA*

(Received 30 January 1986; in revised form 17 April 1986)

Abstract

A single-parameter logarithmic equation is suggested for the calibration of the potential drop method for measuring crack length in compact tension specimens. This equation follows the correct asymptotic solution for long crack lengths and is shown to hold for even very short crack lengths for specimens with a small notch. Use of this equation provides a first step towards evaluation of calibration data for anomalies such as those associated with variation of electrical conductivity due to plasticity of the crack tip and with uneven crack growth. In addition, use of this equation as a two-parameter model allows determination of the electrical resistivity of the specimen from the calibration data. Data are presented for specimens with large notches which support the results obtained in a previous paper by a numerical method coupled with conformal mapping.

Notation

Italic characters

a	crack length, mm (see Fig. 1)
c_k	adjustable parameters for [1], [2], or [3]
d	specimen thickness, mm (see Fig. 1)
h	distance given by 1.25 W in Fig. 1, mm
i	current density, A/m^2
j	$\sqrt{-1}$
R	half-cell resistance, ohms
V	potential drop, V
V_a	potential drop measured for crack length a, V
V_{ao}	potential drop measured for a reference crack length ao, V
W	distance defined in Fig. 1, mm
z_c	crack length, mm (see Fig. 2a)
z_h	cell height, mm (see Fig. 2a)
z_k	height of electrode for resistance measurement, mm (see Fig. 2a)
z_l	length of half-cell, mm (see Fig. 2a)
z_m	half-width of starter-crack notch, mm (see Fig. 2a)
z_n	width of electrode for resistance measurement, mm (see Fig. 2a)
z_u	depth of starter-crack notch, mm (see Fig. 2a)

Greek characters

α	angle at corner of electrode and insulating wall
β	angle of notch (see point D in Fig. 2a)
κ	conductivity, siemens/m
ξ	dimensionless length of uncracked ligament (see [3a])
ρ	resistivity, $\mu\Omega \cdot m$
Φ	electrical potential, V

Subscripts
i imaginary
r real

1. Introduction

The measurement of an AC or DC potential drop across a region of local stress has become a standard method for determining the crack length in metal specimens [1–8]. This technique provides a continuous and nondestructive determination of crack length; however, the interpretation of these data generally requires a separate calibration. For many specimen geometries, analytical solutions of Laplace's equation can be obtained which provide theoretical relationships among variables such as specimen geometry, measured potential drop, and crack lengths [9–12]. Such analytical solutions can guide and support the calibration procedure but are not available for the compact tension specimen geometry. Ritchie and Bathe [13] and Aronson and Ritchie [14] have obtained numerical solutions of Laplace's equation for the compact tension specimen through application of finite element analysis. Accurate use of finite element solutions of Laplace's equation for this system requires, however, a large number of nodes due to the singularities observed at the electrode edges. Orazem [15] has presented a numerical solution of Laplace's equation for this specimen geometry which alleviates this problem through use of conformal mapping coupled with a numerical technique. The objective of this work is to show the application of Orazem's results [15] to the potential drop method for compact tension specimens.

In practice, calibration curves are generally given in the form of V_a/V_{ao} versus a/W where V_a is the potential drop across a specimen with crack length a (see Fig. 1) and V_{ao} is the reference potential drop for a specified value of a. Through the use of such nondimensional terms, the calibration curve becomes independent of the conductivity and thickness of the specimen and of the magnitude of the current. For a given specimen geometry, the calibration procedure involves obtaining an independent measure of the

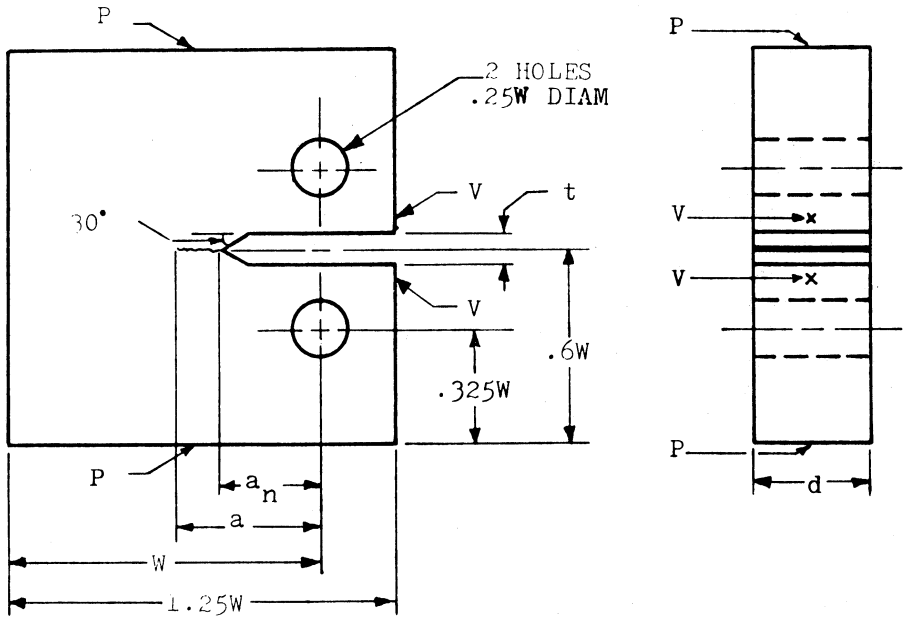

Figure 1. Schematic representation of a compact tension specimen. The locations of current inputs are represented by P, and the location of voltage measurement leads are represented by V.

crack length through such methods as machining a crack to a specified depth, surface observation and measurement of the growing crack, marking the crack length by tinting or overloading, or use of an electrical analog, e.g., graphitized paper or aluminum foil where the crack length can be increased by cutting with a razor blade. The data obtained in this manner are then fit to a three parameter equation such as a power law model with the form

$$\frac{V_a}{V_{ao}} = C_1 + C_2\left(\frac{a}{W}\right)^{C_3} \tag{1}$$

or a two parameter model such as

$$\frac{V_a}{V_{ao}} = C_1 \exp\left[\frac{1}{C_2}\left(\frac{a}{W} - \frac{a_o}{W}\right)\right] \tag{2}$$

where C_k are adjustable parameters obtained by a linear regression of the appropriate

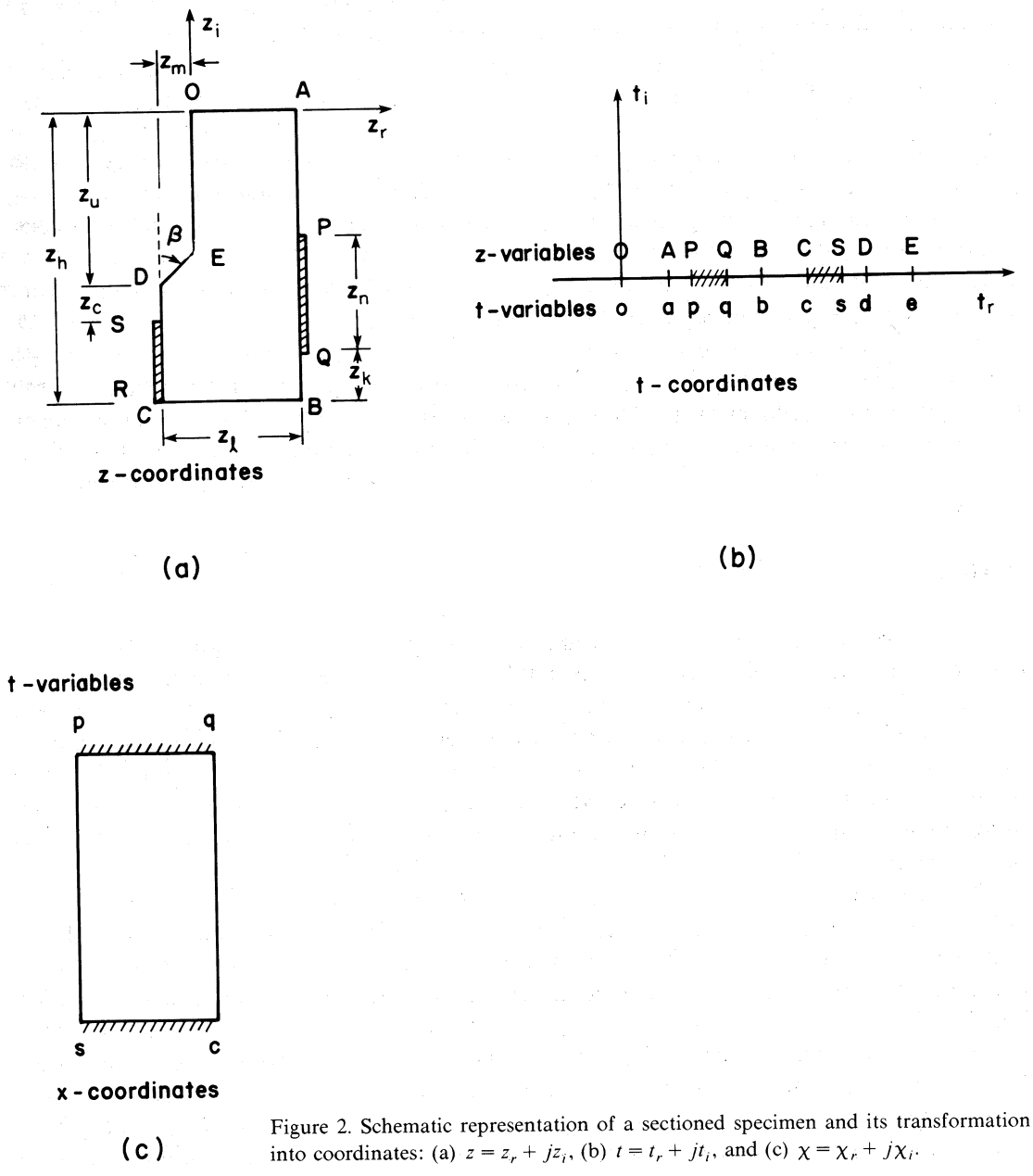

Figure 2. Schematic representation of a sectioned specimen and its transformation into coordinates: (a) $z = z_r + jz_i$, (b) $t = t_r + jt_i$, and (c) $\chi = \chi_r + j\chi_i$.

equation to the calibration data. These equations provide a good match to the calibration data but do not follow the correct asymptotic behavior at long crack lengths, a region where exact knowledge of the crack length is critical. Orazem [15] has suggested that the proper variable for this calibration is

$$\xi = (1 - a/W)\frac{W}{h}. \tag{3a}$$

This variable represents the uncracked length of the specimen normalized by the specimen height h given by 1.25W in Fig. 1. Equation (3a) is consistent with $\xi = (z_h - z_u - z_c)/z_h$ as given in [15] where the length terms are defined in Fig. 2a. The proper form for the calibration curve was suggested to be [15]

$$d\kappa R_1 = C_1 - \frac{4}{\pi}\ln(\xi), \tag{3b}$$

where $d\kappa R_1$ is the dimensionless resistance of the test specimen between the voltage probes related to the usual ratio of potential drop measurements by

$$d\kappa R_1 = \frac{V_a}{V_{ao}} V_{ao}\frac{d}{\rho I}. \tag{3c}$$

These expressions are based upon the asymptotic solution for long crack lengths. With accurate measurement of the current I, the specimen thickness d, and the resistivity ρ, [3] provides an accurate form for the calibration curve with only one adjustable parameter. In addition, for the usual specimen geometry this parameter is very close to zero. If the specimen resistivity is not known, (3) may be regarded to be a two-parameter model from which a value for the specimen resistivity can be obtained.

While (3) provides the correct asymptotic solution for long crack lengths, the degree to which it applies to short crack lengths is perhaps surprising. The experimental verification of this approach is presented in this paper along with treatment of the conditions under which (3) does not apply. A brief discussion of the theoretical method is presented below. Readers interested in the application of these results may skip to the section **Results and discussion.**

2. Theory

Primary current and potential distributions apply to systems for which the surface overpotential can be neglected and the phase adjacent to the electrode has a uniform potential. These assumptions are strictly valid for solid conductors in which the current is electronic. Calculation of the primary current and potential distributions involves solution of Laplace's equation, $\nabla^2\Phi = 0$, which is not trivial, even for simple geometries. The method of images [16], separation of variables [17], and superposition [18,19] have been used to solve Laplace's equation for a number of systems. A review of analytic solutions has been presented by Fleck [20].

The Schwartz-Christoffel transformation [21–23], a type of conformal mapping, provides a powerful tool for the solution of Laplace's equation in systems with planar boundaries. The Schwarz-Christoffel transformation has been used to obtain the primary resistance of a number of cell geometries with application to electrochemical processes [24–27]. This method was used by Moulton [28] to derive the current and potential distribution for two electrodes placed arbitrarily on the boundaries of a rectangle. Moulton's solution provides an asymptotic solution for compact tension specimens with a small notch size. Theoretical calibration curves for fracture specimens have also been obtained through application of conformal mapping for a number of simple specimen

geometries, such as center and edge-cracked plates with various starter notch or crack configurations [9–11]. These are reviewed by Halliday and Beevers [12]. Application of the Schwarz-Christoffel transformation is generally limited, however, by the difficulty of generating solutions to the resulting integrals. Analytic solutions allow calculation of the primary current and potential distributions throughout the cell, but are possible for a limited number of system geometries. Numerical evaluation of these integrals allows calculation of both the primary current distribution along the electrodes and the cell resistance. Orazem [15] has applied this method to the compact tension specimen.

3. Method of solution

The geometry of a compact tension specimen for measurement of crack growth in response to fatigue is presented in Fig. 1. The dimensions are according to ASTM standards for specimen design and are included within the figure. These standards are modified for the study of crack growth in response to steady tension. The envelope of the starter notch is typically small and the angle β is generally $\pi/6$ (30°). This study will also make use of a large notch with angle β equal to $\pi/2$ (90°) to illustrate a region where the numerical results of Orazem [15] apply. Specimens with large notches have been used in stress-corrosion cracking experiments to allow the solution properties near the growing crack tip to be probed. Under the ASTM standards, the test block must be sufficiently thick that edge effects do not influence the propagation of the crack as a plane. This requirement is consistent with analysis of the electrical resistance of this system as being that of a two-dimensional specimen of the shape presented in Fig. 1 and of thickness d.

Under the assumption that current inputs and voltage measurement probes are placed directly opposite each other, the plane of crack growth can be regarded to be a plane of symmetry. Thus the specimen will have twice the electrical resistance of the system presented in Fig. 2a, where constant potential surfaces are designated by RS and PQ and all other boundaries are considered to be insulating. The pin holes (see Fig. 1) were assumed to be filled by a close-fitting pin with the conductivity of the test specimen. The specimen is placed in a complex coordinate system such that the line OA lies on the real-z axis. The coordinate system of Fig. 2a is transformed through an intermediate half-plane t (see Fig. 2b) to a coordinate system (Fig. 2c) in which Laplace's equation can be solved easily.

The primary current distribution along the electrodes and the cell resistance can be calculated through application of the Schwartz-Christoffel transformation. Complex coordinate systems are used, thus

$$z = z_r + jz_i.$$

The z-coordinate system is related to the t-coordinate system of Fig. 2b by

$$z = \int_0^t \frac{(e-t)^{\beta/\pi}}{t^{1/2}(a-t)^{1/2}(b-t)^{1/2}(c-t)^{1/2}(d-t)^{\beta/\pi}}\,\mathrm{d}t, \tag{4}$$

where a, b, c, d, and e are the values of t corresponding to z values of A, B, C, D, and E, respectively. The outside angle at D is represented by β such that $\beta/\pi = 1/2$ for a right angle corner. The electrodes PQ and CS correspond to pq and cs in the t-plane.

The variable χ (see Fig. 2c) is related to the t-variables by the Schwarz-Christoffel transformation;

$$\chi = \int_0^t \frac{1}{(t-p)^{1/2}(q-t)^{1/2}(c-t)^{1/2}(s-t)^{1/2}}\,\mathrm{d}t. \tag{5}$$

Solution of Laplace's equation for the χ-system yields the potential as a linear function of χ;

$$\Phi = \frac{\chi_i}{\chi_{i,\max}} V, \tag{6}$$

where $\chi_{i,\max}$ is the separation between electrodes *cs* and *pq* in the χ-system, and V is the potential difference between the electrodes. The potential drop in the original cell of Fig. 1 is $2V$. The current density is related to the potential derivative at the electrodes. The relationships among the potential derivatives at the electrodes in the χ, t, and z-coordinate systems are developed elsewhere. These relationships are the basis for a system of nonlinear integral equations that can be solved to obtain the current density along either electrode in the z-coordinate system. The dimensionless primary resistance, $d\kappa R$, is obtained through integration over the electrode *pq* in the t-coordinate system:

$$d\kappa R = \frac{2\chi_{i,\max}}{\int_p^q (t-p)^{-1/2}(q-t)^{-1/2}(c-t)^{-1/2}(s-t)^{-1/2}\,\mathrm{d}t_r}. \tag{7}$$

The derivation of [7] and the numerical method used in this calculation are presented by Orazem [15]. The dimensionless electrical resistance is a function of the angle β, three geometric ratios associated with cell shape (e.g., z_l/z_h, z_m/z_h, and z_u/z_h), and three geometric ratios associated with electrode placement (e.g., z_k/z_h, z_n/z_h, and z_c/z_h). In the limit of the starter envelope area approaching zero, the electrical resistance approaches that of a rectangle with appropriately placed electrodes. The solution for this problem has been presented by Moulton [28] in terms of tabulated elliptic functions [29].

The dimensionless resistance calculated in this way is that for the entire specimen. This total resistance consists of the sum of individual resistances in the specimen. The calculated resistance $d\kappa R$ is therefore related to that obtained from the measured potential drop $d\kappa R_1$ by

$$d\kappa R = d\kappa R_0 + d\kappa R_1 \tag{8}$$

where $d\kappa R_0$ is the dimensionless resistance obtained from the potential drop between the current inputs and the leads for potential drop measurement. The term $d\kappa R_0$ may be expected to be independent of crack length for specimens with a large notch size.

4. Results and discussion

The theoretical results of Orazem [15] cannot be applied directly to the calibration of compact tension specimens for which the potential drop is measured at locations different than the current inputs. Aronson and Ritchie [14] state that the top surface close to the notch is the preferred location for positioning leads for measurement of potential differences across the cracked region. This location minimizes errors associated with the uncertainty of probe location and with contact resistances associated with the current inputs. The resistance obtained as a function of crack length with leads separated from the current inputs can be related to the work of Orazem [15] under the assumption that the residual resistance is independent of crack length. This assumption is valid for specimens with a large notch area. The analysis of this method is therefore presented in terms of the influence of notch size and the applicability of [3] as a calibration curve for specimens with a small notch size.

4.1. The influence of notch size

The potential drop method was calibrated by optical measurement of the growing crack on the surface of a specimen subject to fatigue. The optical method was chosen because it is the most commonly applied technique for *in-situ* crack length measurements. Interpretation of the calibration curve obtained through the coupling of the optical and potential drop methods illustrates the type of information which can be obtained from these experiments. The potential drop was measured between leads located at position V and between current inputs located at position P (see Figs. 1 and 3). The current was held at 50 Amps, and the magnitude of the potential drop measured across the notch ranged from 0.5 to 2 mV. The potential drop measured between current inputs ranged from 6 to 10 mV. The potential drop measured between current inputs had a significant contribution associated with the contact resistance and a significant amount of scatter due to the variation of the contact resistance with the tension applied to the specimen. These data were therefore discarded, and the analysis was based upon the potential drop measured between the potential leads as shown in Figs. 1 and 3.

Calibration data are presented in Fig. 4 for specimens with large rectangular notches (see Fig. 3). These specimens were constructed by precracking the specimen with a narrow notch by fatigue and subsequently machining the large notch. Data are presented for notch widths of 8.2, 25.4, and 40.6 mm. The results of numerical calculations for these geometries are presented as solid lines in Fig. 4. The upper dashed line is the asymptotic solution given by Moulton [28]. The calculated resistance is higher than that obtained from the experiments because the data represent the resistance between potential leads,

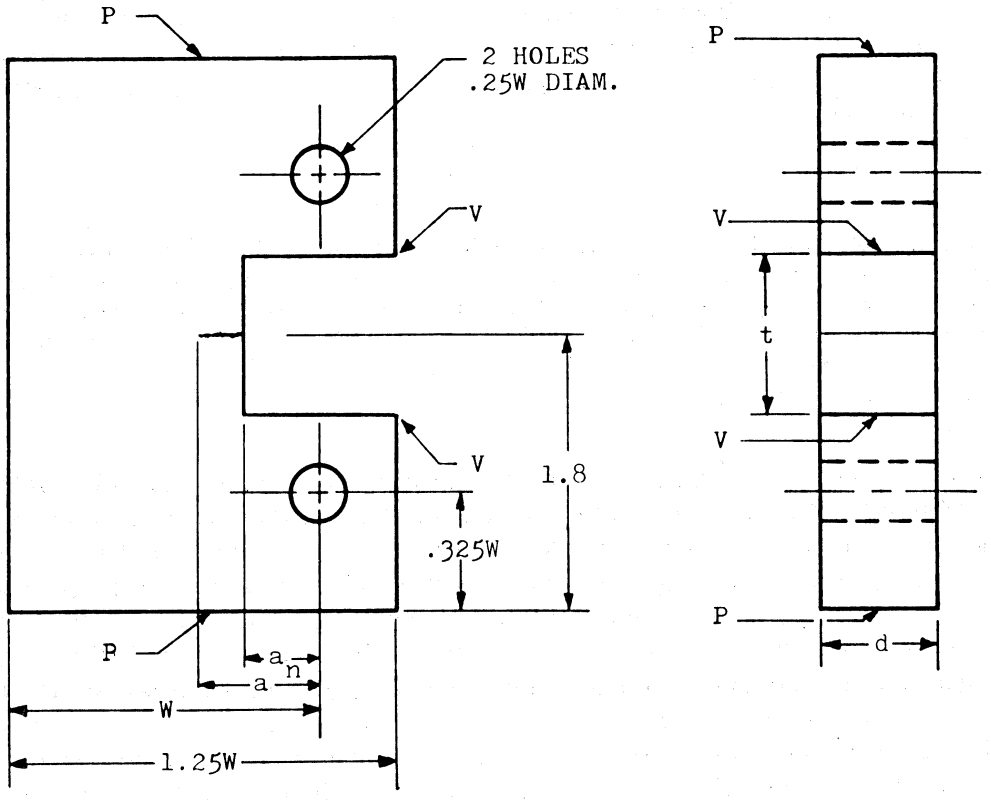

Figure 3. Schematic representation of a compact tension specimen with a large notch. The locations of current inputs are represented by P, and the location of voltage measurement leads are represented by V.

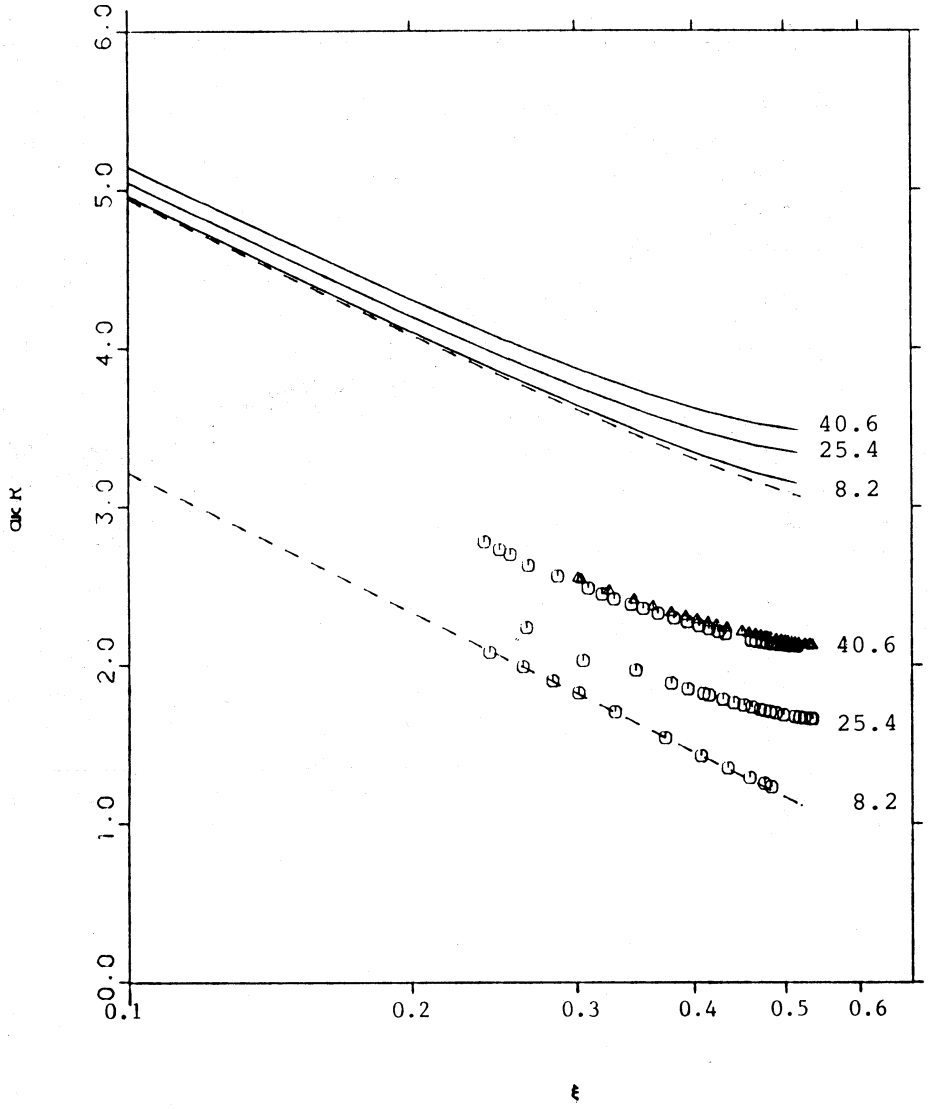

Figure 4. Dimensionless resistance of the specimen of Fig. 3 as a function of the dimensionless crack length variable defined in (3a) with notch size as a parameter. Solid lines are the calculated values from (7), the upper dashed line is the calculated values obtained from Moulton's solution, and the lower dashed line is obtained from (3). All data are for a 7075-T6 aluminum alloy; the different symbols for the largest notch indicate repeated experiments.

whereas the calculations provide the resistance of the entire specimen. Under the assumption that the residual resistance is independent of crack length, the data can be adjusted according to (8). These adjusted data are presented in Fig. 5. The assumption that $d\kappa R_0$ is independent of crack length is strictly valid for large notches, but fails for the smaller notch as shown in Fig. 5. The results presented in Fig. 5 provide experimental verification for the numerical results of Orazem [15] for large notch sizes and support his conclusion that small notches provide optimal sensitivity of the potential drop method to crack lengths.

The results for the specimen with the smaller notch indicate that the residual resistance is a function of crack size for small notches such that the asymptotic solution for long cracks is followed even for short cracks. This result is perhaps both surprising and fortuitous. The simple form of the asymptotic solution for long crack lengths, valid in a

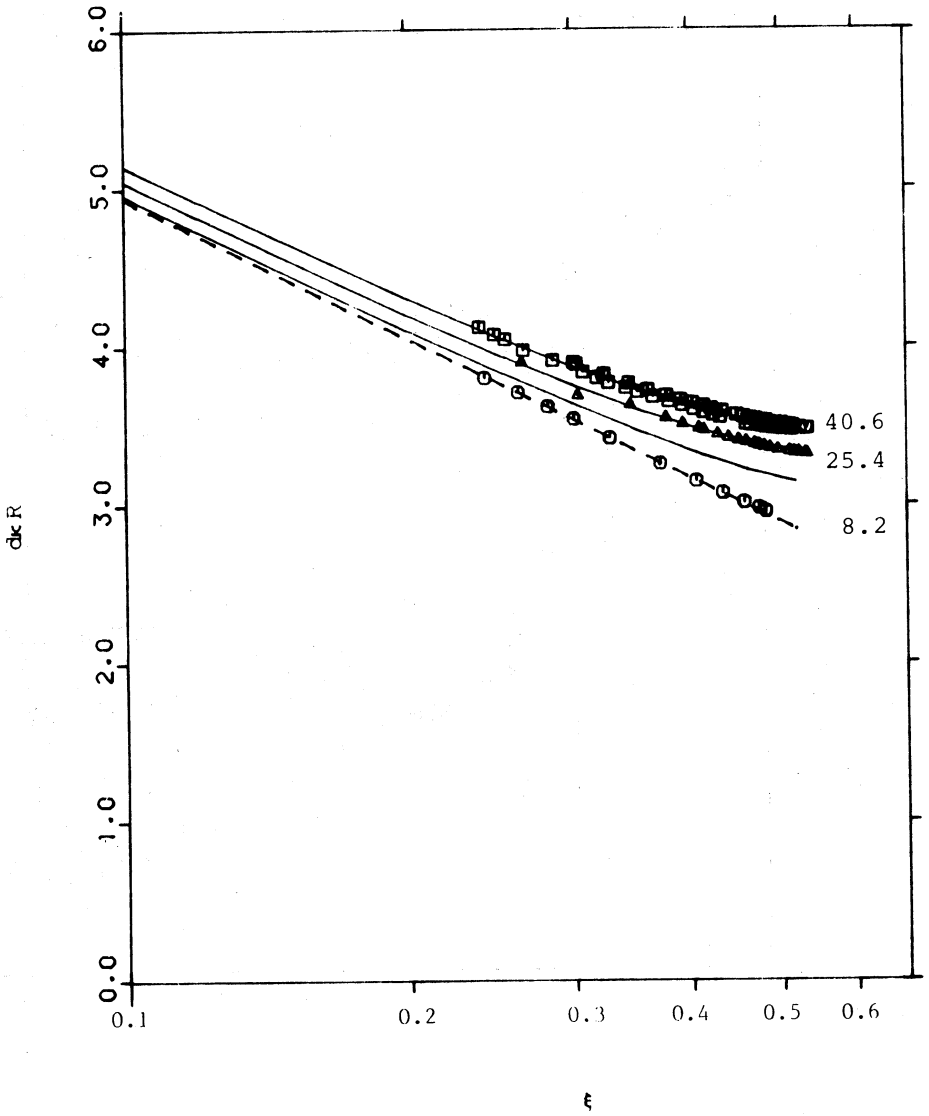

Figure 5. Dimensionless resistance of the specimen of Fig. 3 as a function of the dimensionless crack length variable defined in (3) with notch size as a parameter. Solid lines are the calculated values from (7), and the dashed line is the asymptotic solution for long crack lengths. All data are for a 7075-T6 aluminum alloy; notch sizes are ○ 8.2 mm, △ 25.4 mm, and □ 40.6 mm, respectively.

region where knowledge of the crack length is critical, also applies for small crack lengths under the conditions that the potential drop is measured close to the notch and that the notch is small. These are precisely the optimal specimen configurations suggested by Aronson and Ritchie [14] and by Orazem [15].

4.2. Calibration procedure

Experimental calibration data are presented in Fig. 6 for three specimens of experimental aluminum-lithium-magnesium alloys with small notches as shown in Fig. 1. These alloys were obtained by a mechanical alloying process, and they differ only in carbon content. The solid line is the calculated value for this geometry which follows exactly Moulton's solution [28]. The data most closely follow the asymptotic solution for long crack lengths. The relationship between these data and the traditional method for analysis of calibration

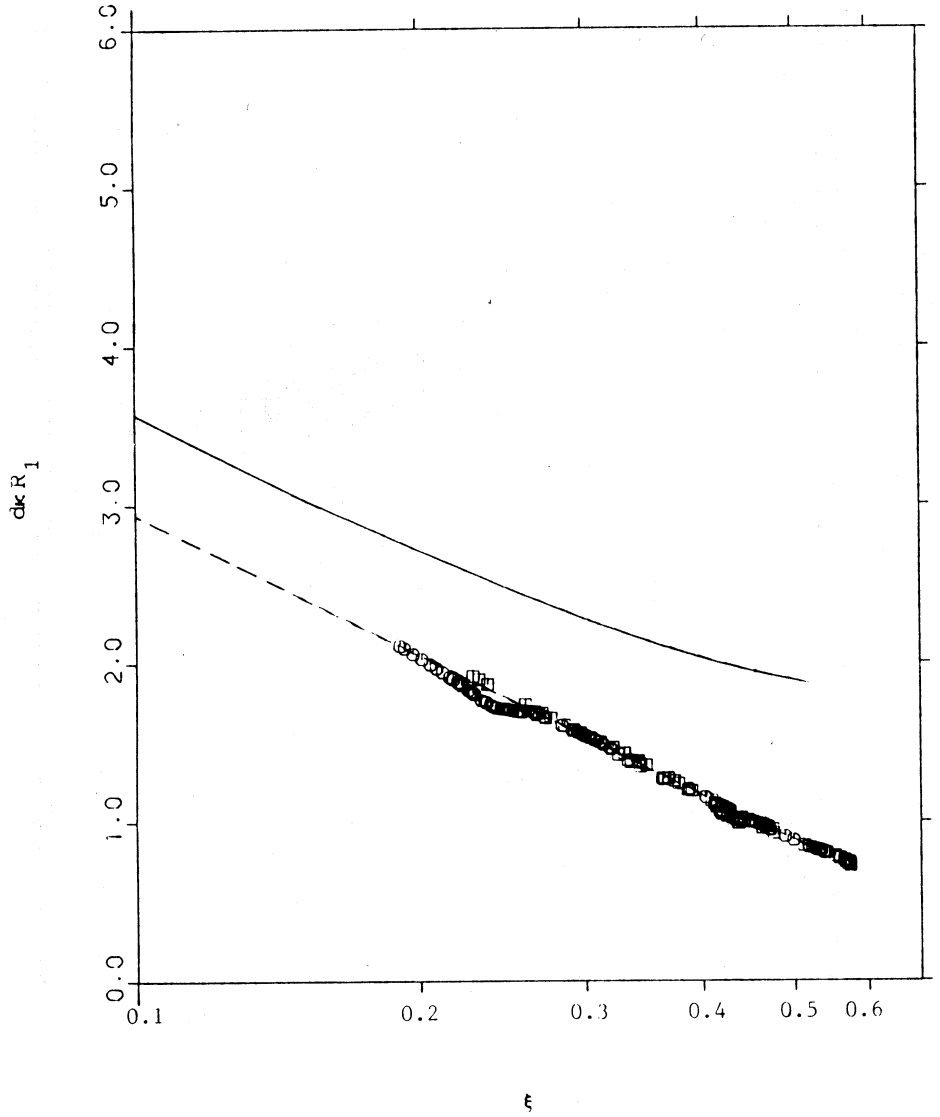

Figure 6. Dimensionless resistance of the specimen of Fig. 1 as a function of the dimensionless crack length variable defined in (3). The solid line is the calculated values from (7), and the dashed line is obtained from (3). □ and △, repeated experiments for an A1-2.5Li-2.0Mg-1.1C-0.60 alloy; and ○ an Al-2.5Li-2.0Mg-0.7C-0.60 alloy.

data as described in the introductory section is seen in Fig. 7. The dashed curve is the best fit according to (2). Equation (3) was used in this analysis as a two-parameter model from which the electrical resistivity for the specimens was obtained. The resistivity was found to be 0.159 $\mu\Omega \cdot$ m for the specimen denoted by triangles, 0.174 $\mu\Omega \cdot$ m for the specimen denoted by squares, and 0.155 $\mu\Omega \cdot$ m for the specimen denoted by circles. The solid line follows (3) where the constant C_1 was equal to 0.097, 0.029, and 0.019, respectively. Independently measured values of the resistivity for these specimens were 0.142, 0.142, and 0.140 $\mu\Omega \cdot$ m, respectively. The first two values are for the same alloy; the deviation between resistivities obtained through the calibration data and the independent measurements can be attributed in part to uneven growth of the crack front. Deviation was most pronounced for samples which showed extensive curvature of the crack fronts. The extent of curvature was observed by examining the overload markings on the fracture surface. The specimen used for the large notch studies was a 7075-T6 aluminum alloy. The

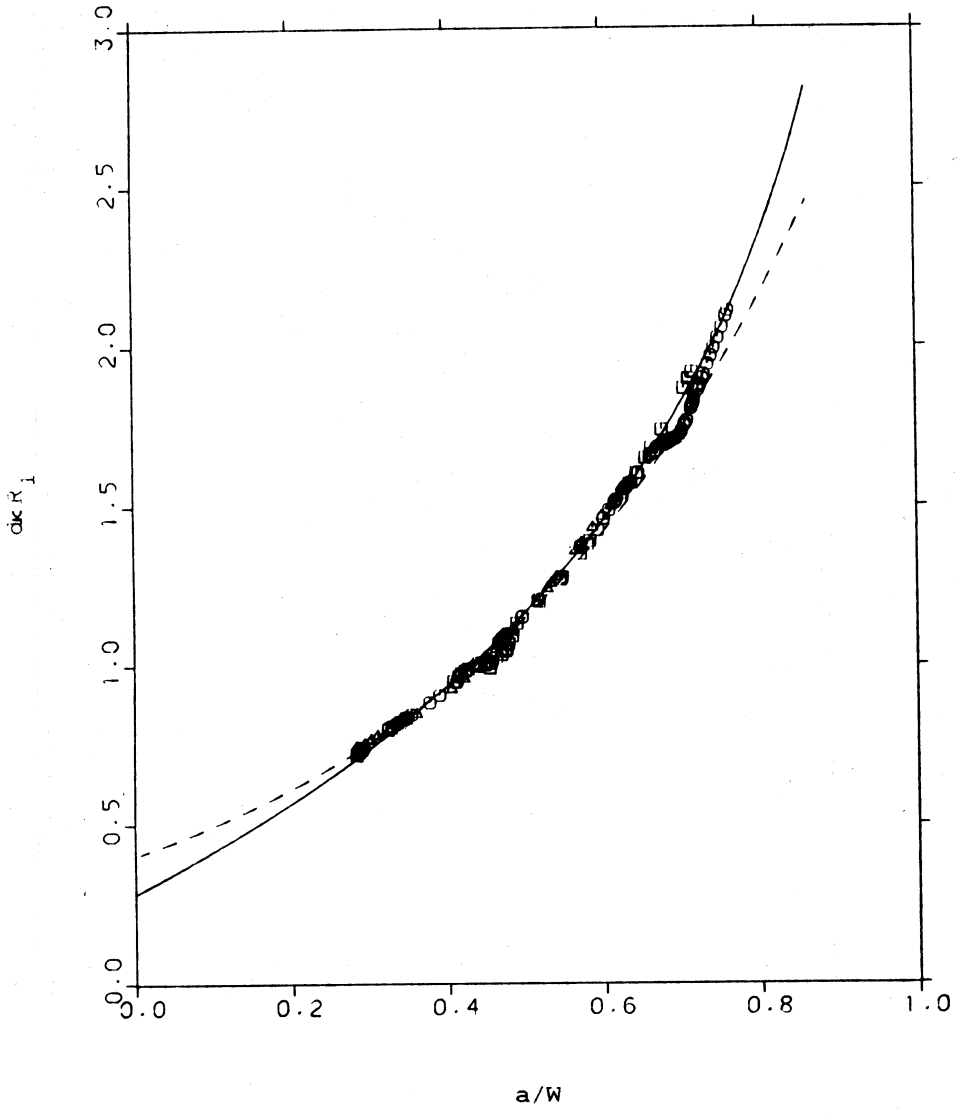

Figure 7. Dimensionless resistance of the specimen of Fig. 1 as a function of a/W. Solid lines are the calculated values from (3), and the different symbols indicate repeated experiments.

electrical resistivity obtained from the calibration data for this material was 0.0641 $\mu\Omega \cdot$ m, and the independently measured value for this specimen was 0.059 $\mu\Omega \cdot$ m. The scatter of data for the calibration of large-notch specimens was smaller; however (3), from which the resistivity was determined, could only be used for the specimen with a smaller notch. This is apparent in the presentation in Fig. 8 of calibration data for specimens with a large notch.

These results show the power of this approach in analyzing calibration data. As a two-parameter model, the calibration data can provide a value for the electrical resistivity of the specimen. This may prove to be especially useful for experimental alloys for which literature values are not available. The shape of the calibration curve is based upon fundamental principles, and the additive constant merely shifts the curve up or down. This is evident in the analysis of the data for large notch specimens as shown in Fig. 8. The model curves shown as solid lines in Fig. 8 differ only in the value for the additive constant. Through this analysis, coupling of the electrical resistance method with other techniques for monitoring crack length provides a first step toward evaluation of such

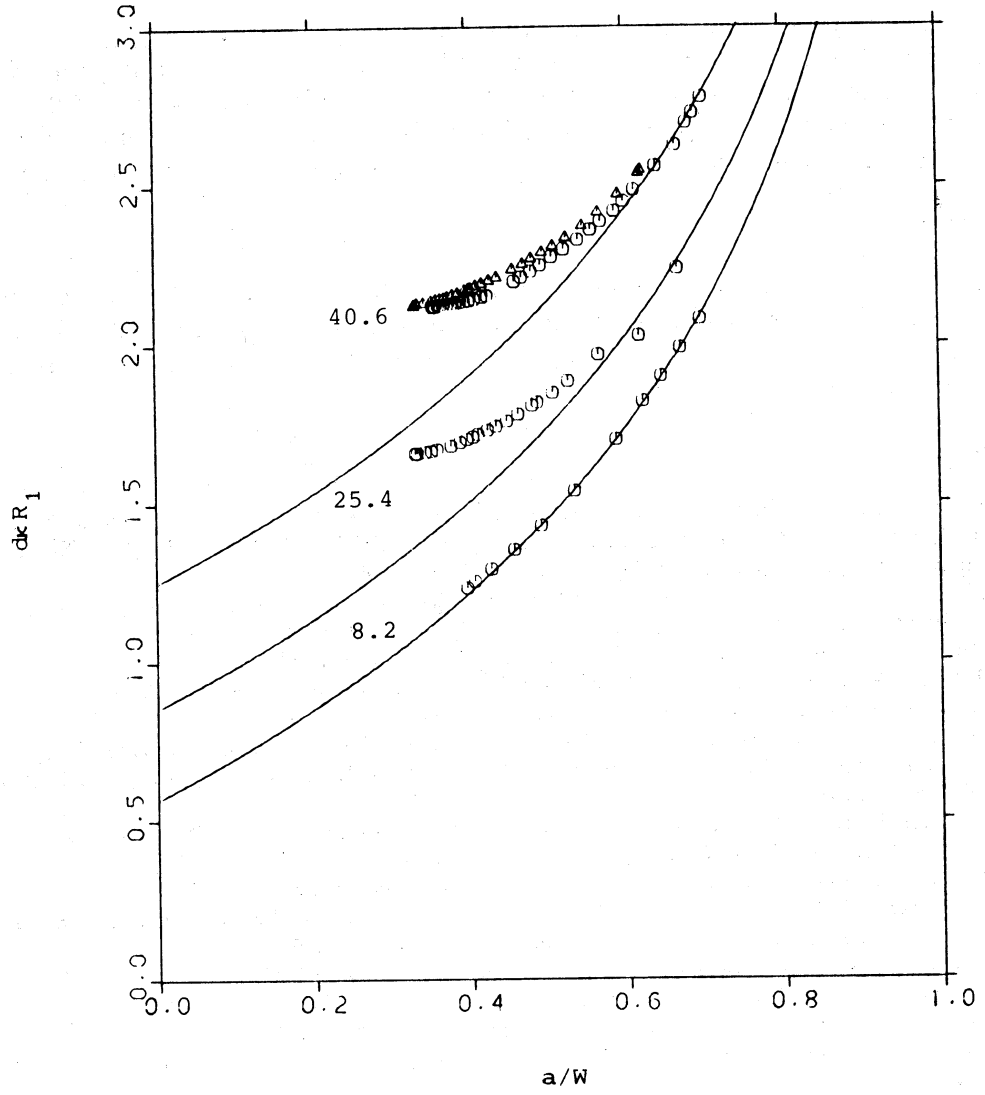

Figure 8. Dimensionless resistance of the specimen of Fig. 3 as a function of a/W with notch width as a parameter. Solid lines are the calculated values from (3), and the different symbols for the largest notch indicate repeated experiments.

anomalies as uneven crack growth, crack closure, and changes in the electrical conductivity near the growing crack tip. Comparison of the data presented in Fig. 7 to the solid line, for example, shows such an anomaly. Uneven crack growth was observed in these tests and is probably responsible for these results. At this point, the method of analysis presented here allows identification of anomalous data, but does not permit definition identification of the responsible phenomena. More work is needed to establish a technique capable of this type of analysis.

5. Conclusion

Equation (3) provides a useful tool for the calibration of the potential drop method for measuring crack lengths in compact tension specimens of the usual dimension. This equation follows the correct asymptotic solution for long crack lengths and holds for even very short crack lengths for specimens with a small notch. For this reason, (3) can be used to evaluate the calibration data for anomalies such as those associated with uneven crack growth, crack closure, and changes in conductivity near the crack tip. Equation (3) can

also be used as a two-parameter model from which the electrical resistivity of the specimen can be determined. The data presented here for specimens with large notches support the results of Orazem [15] obtained by a numerical method coupled with conformal mapping and support the conclusion [14,15] that the optimal specimen geometry includes potential measurement at the top of the specimen across a small notch.

Acknowledgements

This material is based on work supported in part by the Air Force Office of Scientific Research, United States Air Force Systems Command, grant #AFOSR-83-0061, Dr. Alan Rosenstein, program manager (W.R.) and by the Center for Innovative Technology, grant #CIT-MAT-85-027 (M.E.O.).

References

[1] "Standard Test Method for Plane-Strain Fracture Toughness of Metallic Materials", in *Annual Book of ASTM Standards, Part 10*, American Society for Testing and Materials, Philadelphia, PA (1979) 540–561.
[2] W.J. Barnett and A.R. Troiano, *Journal of Metals 9* (1957) 486–494.
[3] R.M. Tchorzewski and W.B. Hutchinson, *Metallurgical Transactions 9A* (1978) 1113–1124.
[4] C.A. Stubbington and S. Pearson, *Engineering Fracture Mechanics 10* (1978) 723–756.
[5] C.J. Beevers, R.J. Cooke, J.F. Knott, and R.O. Ritchie, *Metal Science 9* (1975) 119–126.
[6] N.A.J. Blades, W.J. Plumbridge, and D. Sidey, *Materials Science and Engineering 26* (1976) 195–207.
[7] H.H. Johnson and A.M. Willner, *Applied Materials Research 4* (1965) 35–40.
[8] E.M. Hackett, J.R. Scully, and P.J. Moran, "Influence of Cathodic Polarization on the Fracture Properties of High Strength Steels in Seawater", presented at the Meeting of the Electrochemical Society, Washington, D.C., October 13, 1983.
[9] A.J. Carlsson, *Transactions of the Royal Institute of Technology, Stockholm, Sweden 189* (1962) 1–55.
[10] H.H. Johnson, *Materials Research and Standards 9* (1965) 442–445.
[11] G. Clark and J.F. Knott, *Journal of Mechanics and Physics of Solids 23* (1975) 265–276.
[12] M.D. Halliday and C.J. Beevers, in *The Measurement of Crack Length and Shape During Fracture and Fatigue*, C.J. Beevers, editor, Chameleon Press, Ltd., London (1980) 85–103.
[13] R.O. Ritchie and K.J. Bathe, *International Journal of Fracture 15* (1979) 47–55.
[14] G.H. Aronson and R.O. Ritchie, *Journal of Testing and Evaluation 7* (1979) 208–215.
[15] Mark E. Orazem, *Journal of the Electrochemical Society 132* (1985) 2071–2076.
[16] Charles Kasper, *Transactions of the Electrochemical Society* (1940) 353–384; *78* (1940) 131–160; *82* (1942) 153–184.
[17] John Newman, *Journal of the Electrochemical Society 113* (1966) 501–502.
[18] Joseph J. Miksis, Jr., and John Newman, *Journal of the Electrochemical Society 123* (1976) 1030–1036.
[19] Peter Pierini and John Newman, *Journal of the Electrochemical Society 126* (1979) 1348–1352.
[20] R.N. Fleck, *Numerical Evaluation of Current Distribution in Electrochemical Systems*, M.S. thesis, University of California, Berkeley, September (1964) (UCRL-11612).
[21] Ruel V. Churchill, *Complex Variables and Applications*, second edition, McGraw-Hill Book Company, New York (1960).
[22] E.T. Copson, *An Introduction to the Theory of Functions of a Complex Variable*, Oxford University Press, London (1935).
[23] F. Bowman, *Introduction to Elliptic Functions with Applications*, John Wiley and Sons, New York (1953).
[24] Fumio Hine, Shiro Yoshizawa, and Shinzo Okada, *Journal of the Electrochemical Society 103* (1956) 186–193.
[25] Carl Wagner, *Plating 48* (1961) 997–1002.
[26] John Newman, in *Electroanalytical Chemistry*, A.J. Bard, editor, 6 (1973) 187–352.
[27] Mark E. Orazem and John Newman, *Journal of the Electrochemical Society 131* (1984) 2857–2861.
[28] H. Fletcher Moulton, *Proceedings of the London Mathematical Society (Ser. 2), 3* (1905) 104–110.
[29] L.M. Milne-Thomson, in *The Handbook of Mathematical Functions*, edited by M. Abromowitz and I.A. Stegun, Dover Publications, New York (1972) Chapter 16–17.

Résumé

On suggère une équation logarithmique à paramètre simple pour l'étalonnage de la méthode de la chute potentielle, applicable à la mesure des longueurs de fissure dans des éprouvettes de traction compactes. Cette

équation est conforme à la solution asymptotique correcte pour les fissures longues, et on montre qu'elle est applicable même pour des fissures très courtes dans la cas d'éprouvette comportant une petite entaille.

L'utilisation de cette équation permet l'évaluation des données d'étalonnage dans le cas d'anomalies telles que celles qui sont associées à une variation de la conductibilité électrique due à la plasticité à l'extrémité de la fissure, et en présence d'une croissance inégale de celle-ci.

En outre, l'utilisation de cette équation comme modèle à deux paramètres permet la détermination de la résistivité électrique d'une éprouvette au départ de données d'étalonnage.

Des données sont présentées pour des éprouvettes à grande entaille. Elles viennent à l'appui des résultats obtenus dans un article précédant par une méthode numérique associée à une représentation conforme.